

FIELD INDUCED SWITCHING IN MULTILAYER RHOMBIC MAGNETIC RINGS

BY

JAMES N. PACELLA

**SUBMITTED TO THE DEPARTMENT OF MATERIALS SCIENCE AND
ENGINEERING IN PARTIAL FULFILLMENT OF THE REQUIREMENTS FOR
THE DEGREE OF**

**BACHELOR OF SCIENCE IN MATERIALS SCIENCE AND ENGINEERING
AT THE
MASSACHUSETTS INSTITUTE OF TECHNOLOGY**

JUNE 2007

Signature of Author: _____

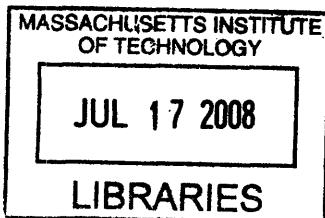
Department of Materials Science & Engineering
May 21, 2007

Certified by: _____

Caroline A. Ross
Professor of Materials Science & Engineering
Thesis Supervisor

Accepted by: _____

Caroline A. Ross
Professor of Materials Science & Engineering
Chair, Departmental Undergraduate Committee



ARCHIVES

FIELD INDUCED SWITCHING IN MULTILAYER RHOMBIC MAGNETIC RINGS

BY

JAMES N. PACELLA

Submitted to the Department of Materials Science and Engineering
On May 21, 2007 in Partial Fulfillment of the
Requirements for the Degree of Bachelor of Science in
Materials Science and Engineering

ABSTRACT

Multilayer rhombic magnetic rings are researched as a structure for the “pseudo spin valve” device that could possibly become useful in magnetic materials applications such as MRAM, digital logic, and sensors through the use of multiple resistance states exhibited within these devices. The magnetization reversal characteristics of these structures are explored in an effort to fully understand interactions occurring within the devices and their resulting effect on giant magnetoresistance (GMR). Contact configuration and angular dependence of applied field are also examined. Using sub-micron thickness rhombic rings with long axis dimension $\sim 1.5\mu\text{m}$, major loop magnetization sweeps were conducted, as well as minor loops in order to excite several resistance states within the devices. It was found from major loop applied field sweeps that rhombic multilayer rings exhibit five stable magnetoresistive states, with an additional state excited through execution of a minor loop field sweep. In addition, using the contact configurations known as “classical” and “wheatstone bridge” provide additional information on interactions that are occurring within the structures. It was found that both contact configurations were sensitive to similar changes in the devices, however, through different means of sensing. The major difference results in a larger GMR output in the wheatstone bridge configuration ($\sim 20\%$) versus the classical configuration ($\sim 1\%$). Preliminary work in angular dependence has shown the ability to alter resistance plateaus by changing the angle of applied field. Ultimately shown through this work is the amount of research that is still needed to truly understand these devices, as they contain more complex stable and metastable states of magnetization than generations and shapes before them.

Thesis Supervisor: Caroline A. Ross
Title: Professor of Materials Science & Engineering

TABLE OF CONTENTS

	<u>Pg.</u>
ABSTRACT.....	2
ACKNOWLEDGEMENTS.....	4
1. INTRODUCTION.....	5
2. BACKGROUND.....	6
2.1. THIN FILM MAGNETIC RINGS.....	7
2.2. PSEUDO SPIN VALVES.....	7
2.3. ELLIPTICAL PSV RINGS.....	8
2.4. APPLICATIONS.....	10
2.4.1. MRAM.....	10
2.4.2. DIGITAL LOGIC.....	10
2.4.3. SENSORS.....	11
3. FABRICATION.....	12
4. MAGNETORESISTANCE IN RHOMBIC MAGNETIC RINGS.....	12
4.1. EXPERIMENTAL PROCEDURES.....	12
4.2. EXPERIMENTAL RESULTS.....	14
4.2.1. EASY AXIS MAGNETIZATION.....	15
4.2.2. COBALT VORTEX SWITCHING.....	17
5. INFLUENCE OF CONTACT CONFIGURATION.....	18
5.1. WHEATSTONE BRIDGE CONFIGURATION.....	19
5.2. WHEATSTONE BRIDGE RESULTS.....	20
5.3. CORRELATION BETWEEN MODELS.....	22
5.4. CONFIGURATION CHARACTERISTICS.....	23
6. ANGULAR DEPENDENCE.....	25
7. CONCLUSION.....	26
REFERENCES.....	28

ACKNOWLEDGEMENTS

I would like to extend a very special thank you to Professor Caroline Ross for all her help and guidance throughout this process. Also, I would like to thank members of the Magnetic Materials and Devices Group: Fernando J. Castano, Irene Colin, and Filip Ilievski, as they were instrumental in helping me achieve my goals. I would also like to thank Phil Zakielarz and Nan Yang for their specific help in much needed areas of this project. Lastly, I would like to thank my friends and family for all their support.

1. INTRODUCTION

Thin film magnetic rings have generated a great deal of interest in recent years due to the existence of multiple stable magnetic states and their possible applications in memory, logic, and sensing devices.¹ To date, elliptical magnetic rings have been researched extensively; however, other shapes are being explored to determine whether device shape can affect magnetic performance. To this end, multilayer rhombic magnetic nanorings have been developed with structural characteristics that could lead to their becoming alternatives for use in thin-film magnetic applications.

Like elliptical rings, rhombic rings exhibit different stable states of magnetization. However, the highly defined shape of these multilayer rhombic structures has allowed researchers to have more control over the microscopic magnetic interactions within the material, yielding a new, stable magnetic state previously unseen in elliptical rings. In recent years, elliptical rings have generated interest due to the existence of flux-closed magnetic configurations ("vortex" states), in which the magnetization travels circumferentially around the ring, either clockwise or counterclockwise.² Now, in multilayer rhombic magnetic rings, we not only see these flux-closed states occur in both the hard and soft magnetic layers, we also see a $\frac{3}{4} - \frac{1}{4}$ magnetization configuration, yielding an additional stable magnetic state. As a result, this novel structure could theoretically lead to an increase in the density of magnetic random access memories.

The physics of multilayer rhombic magnetic rings is, however, more complex than that of elliptical rings, as the shape of the device causes unforeseen magnetic interactions, presenting new challenges. One such challenge is determining the best contact configuration for testing the devices. Multiple contact configurations and their

effect on magnetoresistance measurements have previously been examined for similar thin-film devices;³ however, there has been little work on interpreting the influence of the electrical contact geometry on these multilayer devices. This paper aims to examine two types of contact configurations used in testing multilayer magnetic rings in order to gain knowledge on the interactions within rhombic structures. Section 2 will review background work on multilayer magnetic rings and their applications. Section 3 will describe fabrication of these devices. Section 4 will explain magnetic interactions within rhombic structures and section 5 will explore the influence of contact configuration. Finally, section 6 will look at the angular dependence of these devices as well as future work in the field.

2. BACKGROUND

A great deal of research has been conducted in route to the creation of multilayer rhombic magnetic rings. To truly understand the significance of these devices, we must delve into their long developmental history. Furthermore, in order to understand the rhombic ring's potential, we must also explore the applications and commercial viability of these devices to determine the best course for the future of this technology. Of course, research on many different magnetic materials and configurations is still being researched, largely outweighing that on rhombic structures. Although the rhombic structure may prove to be an interesting alternative or even the next step in this scientific process, its history must be understood in order to interpret its future.

2.1. THIN FILM MAGNETIC RINGS

Thin film ferromagnetic rings were originally researched for their potential applications in memory and sensor devices. In addition, the circular ring structure proved helpful in understanding fundamental properties of domain walls such as resonance, motion, and reproducibility.⁴ In permalloy (Py) rings consisting of $\text{Ni}_{80}\text{Fe}_{20}$, a forward onion, vortex, and reverse onion state, which will be explained in detail below, were found to be both reproducible and controllable.⁴ Cobalt elliptical rings have also been shown to exhibit similar states of magnetization and control over domain walls.⁵

2.2. PSEUDO SPIN VALVES

The multilayer rhombic magnetic rings can be classified as a “pseudo spin valve” structure. A variant of the pseudo-spin-valve (PSV) structure called a spin valve is presently used in multiple varieties of hard disk readback sensors, typically consisting of ferromagnetic layers separated by an anti-ferromagnetic layer. In contrast, a pseudo spin valve consists of two thin-film magnetic layers of different materials (in our experiments we use Co, a hard magnetic material, and NiFe, a soft magnetic permalloy), or two layers of the same material of different thickness, separated by a non-magnetic spacer layer (Cu in our experiments).⁶ In the pseudo spin valve mode of operation, starting from a state where the magnetization directions of both the soft and hard magnetic layers are parallel (usually saturation), as the field is swept in a direction opposing the magnetization of the cell, the cell reacts. The soft/thin magnetic layer switches first, creating anti-parallel magnetic moments with its counterpart. Once the layer has switched, it tends to inhibit switching of the thicker/harder layer.⁷ As field increases, the second layer switches as

well, eventually re-aligning the moments to parallel. When current is passed through a pseudo spin valve device, interactions between magnetic moments within respective layers affect the flow of current through the device. This is known as giant magnetoresistance (GMR) and has become a very desirable attribute of these devices. In magnetic applications, the pseudo spin valve mode is non-destructive read-out (NDRO), exhibits high GMR, and works well for sub-micron cells.⁷

2.3. ELLIPTICAL PSV RINGS

Ferromagnetic ring structures have long been recognized as potentially useful magnetoresistive random access memory (MRAM) devices due to the fact that they exhibit highly stable vortex states in which the magnetization circulates around the structure in one or two possible senses.⁸ This continuous circulation limits stray fields that may be created, enabling the distance between structures to be minimized. Detailed magnetotransport studies of micron-sized Co/Cu/NiFe elliptical rings with widths of 90 nm and above have been conducted by Ross *et al.*⁹ To measure the PSV devices, a constant current of 10 μ A was applied through two contacts of a 4-point probe, measuring

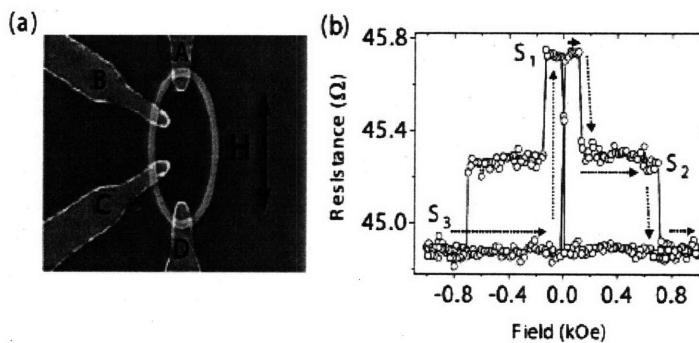


Figure 1. Experimental results from elliptical PSV device. a) SEM Image of PSV multilayer ring. b) Magnetoresistance loop showing three distinct states of magnetization.⁸

the voltage drop across the other two contacts. Inside the ring, the current splits from one electrical contact, traveling equally around half of the ring toward the other contact. The voltage drop measured was

found to be sensitive to the relative angle between magnetizations of the permalloy and hard magnetic layers throughout the ring.⁹ The magnetic field was swept from positive to negative saturation, returning to positive saturation (Fig. 1).

As shown in Fig. 1, while the magnetic field travels to remanence from saturation, both layers of the elliptical PSV structure exhibit parallel magnetic moments in what is known as the forward “onion” state. When the field switches, the soft magnetic layer completely switches to a reverse onion state, having moments completely anti-parallel to the hard Co layer. This state corresponds to the largest resistance plateau in Fig. 1. As the field increases, the Co layer enters the vortex state. This results in half of the structure consisting of parallel magnetic moments while the other half remains anti-parallel. Accordingly, the output resistance is at an intermediate level. Finally, at relatively large fields, the Co layer completely reverses and both layers are in the reverse onion state, completely parallel again. Unlike its single layer counterpart, in the PSV structure, the NiFe layer does not exhibit vortex behavior, but instead completely switches to the reverse onion state at low switching fields. This occurs because the NiFe reversal is dominated by magnetostatic coupling from the domain walls in the Co layer.⁹ In some experiments, over small ranges of applied fields, both the NiFe and Co layers can enter a “twisted onion” state, characterized by the formation of 360° domain walls. Although this state has little effect on magnetoresistance, it has been shown to be present in both experiments and simulations. The formation of these walls plays a major role in the switching between states, in some cases, creating complex, metastable states within the device.²

2.4. APPLICATIONS

Multilayer magnetic rings show great promise in storage and sensing applications. Though there is still work to be done before practicality can be established, these devices could potentially improve the state of technology in three major areas: MRAM, digital logic, and sensor devices.

2.4.1. MRAM

As previously stated, multilayer magnetic rings have generated a large amount of interest due to their potential to increase density in MRAM devices. With multiple, stable magnetic states available in these devices, each multilayer ring could store two or three bits instead of the one bit used in current technology. However, multiple issues would need to be addressed in order to create a practical device.⁸ For example, emitting switching fields that wouldn't affect surrounding rings as well as non-destructively reading the different states in each ring is a primary commercial concern. Current research in this area includes using the spin-torque effect to switch the PSV devices with small bursts of current. This could lead to a more practical device configuration that consumes less power. In addition, the size of individual PSV rings would most likely need to be reduced. Fortunately, research suggests that the size of the device could be significantly reduced while still maintaining functionality.⁸

2.4.2. DIGITAL LOGIC

Digital logic is currently based on the binary number system. Only two states, 0 and 1, true and false, yes and no, create the groundwork for logic functions. One

essential component of this system is creating memory structures that can switch back and forth between two clearly-defined states, with no ambiguity. It is also ideal to design and build circuits that will remain indefinitely in one state unless and until they are deliberately switched to the other state.¹⁰ PSV multilayer rings could theoretically be used as an alternative to present technology. Furthermore, should the basis for logic expand beyond simply two states, these devices could be excellent candidates for a three state structure. Many computer scientists have evaluated and proposed using multiple-valued logic in digital electronics.¹¹ As a result, research is being conducted in multiple areas of materials science to find a structure that can exhibit three stable and distinguishable states.¹² Unfortunately, a practical structure has not yet surfaced as the ideal candidate for this application.¹³ PSV multilayered magnetic rings could be the answer to this problem, as they exhibit at least three stable magnetoresistance states. Like MRAM, the size of the rings would have to be reduced in order to achieve practicality, but as previously stated, it may be theoretically possible.

2.4.3. SENSORS

The use of thin-film magnetic rings as sensors has been proposed, in particular for biosensors.¹⁴ Magnetoresistive sensors could be used to detect the presence of micron-sized magnetic particles that function as bimolecular labels.¹⁵ Using partially magnetized spheres of NiFe, the magnetoresistance response to the generated fringing field is strongly peaked when the sphere is directly above the center of the ring and rapidly decreases to zero when the sphere is outside the ring.¹⁵ Arrays of PSV devices would be a highly efficient device for this application, although careful consideration would need

to be paid to ensure the stability of the vortex circulation state. This feature makes PSV structures especially attractive because they will not produce an external magnetic field.

3. FABRICATION

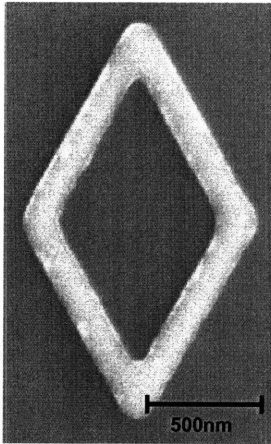


Figure 2. SEM image of PSV multilayer rhombic magnetic ring

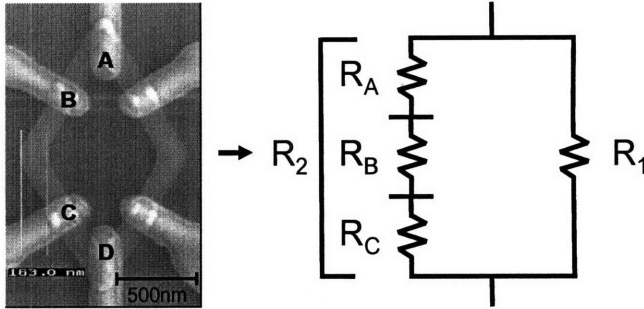
The PSV multilayer rhombic devices of inner dimensions $1.5 \mu\text{m}$ by $0.75 \mu\text{m}$ and widths between 0.15 and $0.2 \mu\text{m}$ were fabricated by electron beam lithography and lift-off processing. The stacks consist of polycrystalline Co, Cu, NiFe, and Au over a substrate. The stack configuration corresponds to $4\text{nm-Co}/4\text{nm-Cu}/6\text{nm-NiFe}/4\text{nm-Au}$ and was deposited by ultrahigh vacuum sputtering. Four electrical contacts with consisting of Ta/Cu layers were overlaid on the ring in a second lithography step. A SEM image of an un-contacted ring is shown in Fig. 2.⁸

4. MAGNETORESISTANCE IN RHOMBIC MAGNETIC RINGS

4.1. EXPERIMENTAL PROCEDURES

PSV multilayer rhombic structures are tested using a 4-point probe technique with a constant rms current of $10 \mu\text{A}$ at a frequency of 14.4 kHz , with ac lock-in detection. The contact configuration used in this procedure is referred to as the “classical configuration”, defined by one current lead at each end of the long axis and two voltage leads measuring the drop between the centers of adjacent arms, shown in Fig. 3.

Resistance is calculated by equating current that travels across either half of the ring, modeled in Fig. 3. Another configuration is also examined, and will be discussed later.



$$V_{12}/I = (R_1 R_B)/(R_1 + R_2)$$

Figure 3. SEM Image of Classical Configuration with Electrical Schematic. The device is modeled as a set of resistors in a circuit. Total resistance is calculated with the resulting equation.³

The devices are placed between the poles of an electromagnet, on a precision rotating stage capable of ensuring accurate angles between the magnetic field and desired axis of the specified rhombic device. Field is manually swept beyond either positive or negative

saturation and then brought back to remanence. Field is then controlled automatically, sweeping first in one direction to saturation (between 400 and 1000 Oe in most experiments), then back to reverse saturation (of same magnitude). The field then retraces its course, first, back to the first saturation field, then to remanence again. Output resistance measurements are represented in a MR loop with units in Ohms. A simple conversion is used to convert MR values into a giant magnetoresistance ratio, defined as $[(R - R_{\min})/R_{\min} \times 100]$.³ The magnetoresistance states of the multilayer rhombic structures will be explained in 4.2, as well as the major interactions that contribute to these results.

4.2. EXPERIMENTAL RESULTS

The rhombic device connected through the classical configuration was tested with an applied field that was swept from +400 to -400 Oe. Fig. 3 shows its corresponding scanning electron micrograph (SEM) as well as the contact configuration. This rhombic device showed a GMR ratio of 1.0% ($\pm 0.1\%$), shown in Fig. 4.

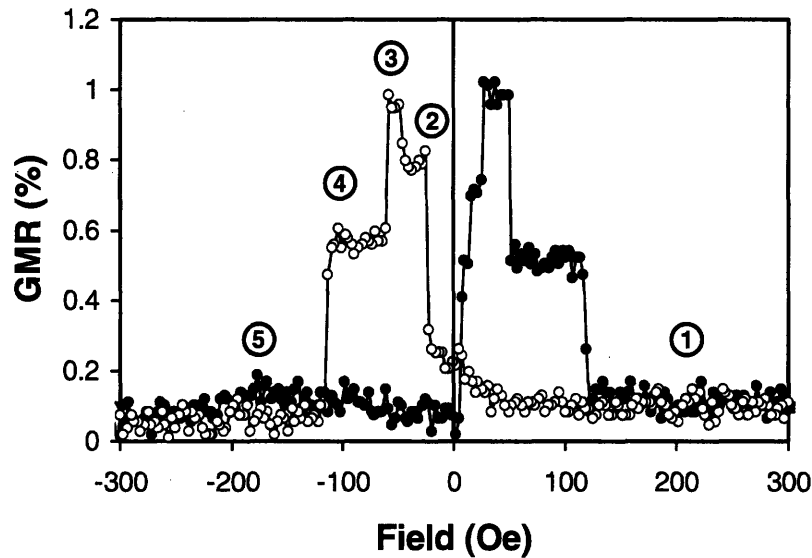


Figure 4. Magnetoresistance Loop in Rhombic Structure. The ring is contacted using the classical configuration and field is swept ± 800 Oe. Resistance plateaus occur due to coupling of magnetic moments between layers of PSV device.

The magnetotransport data displays 4 distinct plateaus with abrupt transitions, labeled accordingly. Starting from saturation (step 1), when the field is reversed, the first transition at low fields occurs, yielding an intermediate resistance state (step 2). This is shortly followed by the transition into the highest resistance state (step 3). As applied field increases, the device switches to another intermediate resistance level (step 4), and then finally to the low resistance state (step 5). The resistance of step 5 is equal to that of step 1, and is identical at positive and negative saturation. Whereas elliptical multilayer rings have shown only three distinct states of magnetization, Fig. 4 suggests that the

rhombic structure's geometry must allow an intermediate step in the permalloy to occur (step 2), though it remains unclear as to why this phenomena is seen in rhombic structures and not in elliptical ones. The underlying magnetic interactions between each resistance plateau are described qualitatively in Fig. 5, as the magnetization of the individual layers of the PSV structure is discussed in 4.2.1.

4.2.1. EASY AXIS MAGNETIZATION

Each individual resistance state is governed by the magnetic interactions within the PSV rhombic structure. From looking at single layer rings, we have shown a multitude of possible states that can occur in these materials. By combining possible interactions between layers and looking at the relative difference in magnetic moment, we can qualitatively determine the magnetic state within each layer, shown in Fig. 5.

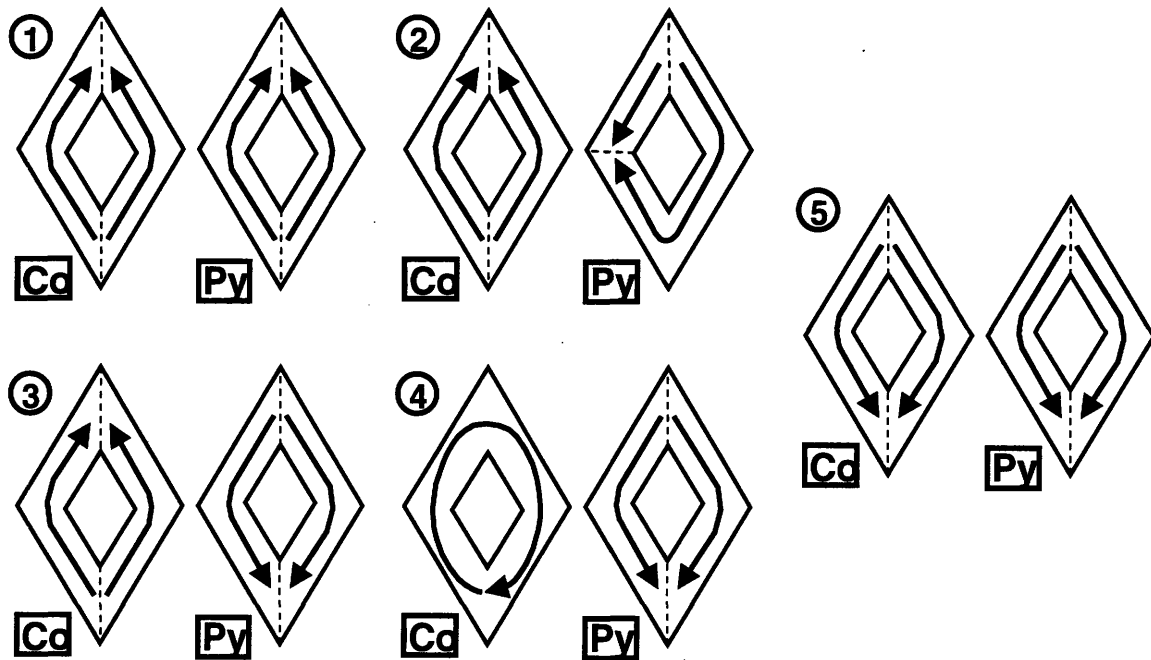


Figure 5. Magnetic Moment Illustrations. Above are predicted and simplified representations of how the magnetic moment should be in each layer to produce a corresponding resistance in Fig. 4.

Next to each number are the most likely magnetic configurations for both the Co and permalloy layer with respect to its resistance level in Fig. 4. In state 1, both the Co and NiFe exhibit the forward onion state with two 180° domain walls, one at either end of the long axis of the rhombic structure.

At the first transition after switching the field (step 2), we see an abrupt jump that is confined to an intermediate resistance level. Similar behavior observed in single layer NiFe rings had been attributed to the permalloy entering a vortex state with the hard magnetic layer remaining unchanged.² This would cause half the ring to have parallel moments while the other half would be anti-parallel, hence, creating an intermediate state. However, this solution poses the problem of having a different resistance level than in step 4, when the cobalt is in the vortex state. Since device magnetoresistance is based on moment coupling between the hard and soft magnetic layers, a NiFe vortex state should yield identical resistance results seen in step 4. Therefore, the logical explanation to this newly observed resistance state is that the moments within the NiFe layer are $\frac{3}{4}$ anti-parallel and $\frac{1}{4}$ parallel with the Co layer. This would account for the higher intermediate state if we think of the vortex to onion coupling as one half the maximum resistance and this state as three quarters. Though the rhombic geometry seems to be the cause for this additional state, it is worth noting that the magnetic configuration of the NiFe layer is not restricted to moments that are confined within straight regions of the rhombic structure. As domain walls grow and propagate through the material, local regions of aligned magnetization can occur at any point and over any distance in the rhombic ring.

4.2.2. COBALT VORTEX SWITCHING

During major loop sweeps, it has proven difficult to excite the permalloy layer into a vortex magnetization state, as opposed to results seen in single layer experiments.² When the material is in a vortex magnetization state, it gives off little to no stray magnetic field, making this state very important in devices that may utilize these PSV structures. Though total sweeps have proven un-effective at exciting this state in the NiFe layer, by maintaining a vortex state within the Co layer and sweeping over minor loops, the NiFe can show vortex circulation at low fields, shown in Fig. 6.

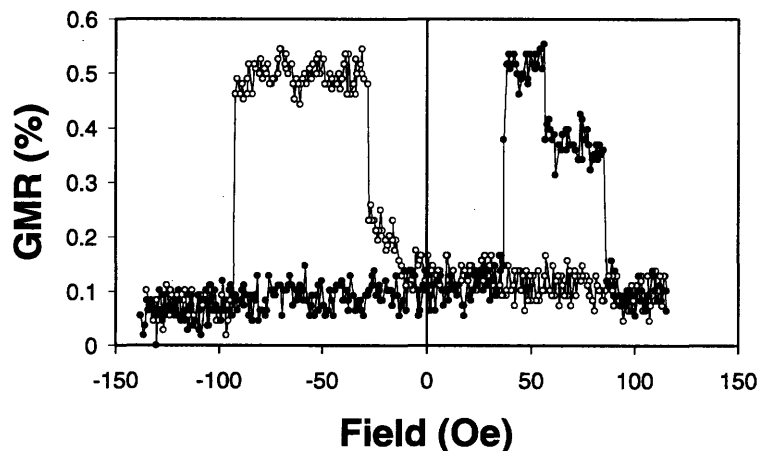


Figure 6. Co Vortex Switching of Permalloy layer. The device is first saturated and then brought back to remanence. A field is applied that reverses the NiFe and forces the Co into a vortex state. The Co layer is then held in the vortex state while minor loops are conducted to induce switching in the NiFe layer only. In this regime, the NiFe switches between a reverse onion (low R) state and a reverse vortex state (high R), with an intermediate step along the way.

In Fig. 6, the baseline corresponds to a Co vortex coupled with a NiFe onion state. In this figure, we see the resistance switch to a high level at approximately -30 Oe. Looking back at Fig. 3, the GMR for this structure was $\sim 1.0\%$ at maximum, with the Co vortex/Py onion state at half-maximum. Therefore, a GMR change of 0.5% for this experiment implies that the NiFe layer is, in fact, anti-parallel to the Co layer, yielding a GMR ratio concurrent with Fig. 4. Since the Co layer is held in a vortex state, the NiFe

must be in a vortex of opposite direction to achieve this result. In addition, at ~60 Oe, the resistance falls from 0.5% to an intermediate level. Recall from Fig. 5 that this level corresponds to a $\frac{3}{4}$ anti-parallel, $\frac{1}{4}$ parallel configuration for the permalloy, consistent with previous data. This gives us important information on the domain wall movement inside the NiFe at low fields, and, more importantly, sheds more light on how the first intermediate stage is formed from Fig. 4. Fig. 6 clearly shows that the permalloy vortex state precedes its $\frac{3}{4}$ and $\frac{1}{4}$ state. Therefore, from saturation and upon switching fields, one of the 180° domain walls (from step 1) must travel across the ring, meeting or annihilating with its counterpart to form either a vortex or twisted vortex with a 360° wall. As field increases, a reverse domain within the material must grow to approximately $\frac{1}{4}$ the area of the rhombic structure, resulting in the intermediate resistance level found at around 80 Oe. Why does this only occur in one direction in this experiment? The answer lies in the probable fact that the NiFe layer was not in a fully developed onion state upon reversing direction towards negative field. This can be seen in the slight slope seen in resistance values from 0 Oe to around -25 Oe when the transition to the vortex state is made, most likely caused by the asymmetrical sweep of the MR loop. In any event, the important aspect of this experiment is that we now know it is possible to excite a stable dual-vortex state in the pseudo spin valve multilayer rhombic structures, one that could have significant value to high-accuracy applications.

5. INFLUENCE OF CONTACT CONFIGURATION

Some work has been conducted to determine an accurate and reliable way to connect PSV multilayer rings and determine transitions between resistance states.

Morecroft *et al.* have evaluated the classical contact configuration for PSV rings to determine the best way to get a valuable measurement.³ Furthermore, Saitoh *et al.* has explored the idea of representing the 4-point probe as a wheatstone bridge (WB) circuit in single layer magnetic rings.¹⁶ However, virtually no work has been conducted to determine the influence of these contact configurations on the performance of the device.

5.1. WHEATSTONE BRIDGE CONFIGURATION

Like its classical configuration counterpart, the wheatstone bridge contact configuration is a 4-point probe measurement that can be used to track changes in magnetoresistance within the multilayer ring. However, this configuration functions slightly differently than the classical configuration. Instead of monitoring the potential drop across a section of the ring and extrapolating the device resistance, this configuration models the rhombic device as a wheatstone bridge, a configuration used to determine small perturbations in resistance, represented in Fig. 7.

As current is passed through opposite ends of the circuit, it must travel through branches with two resistors each: R1-R2 or R3-R4. If the resistances along each branch are symmetrical, that is, if R1 were identical to R3 and R2 identical

to R4, there will be no voltage difference between nodes A and B. However, if one resistor were to independently change, the symmetry of the circuit

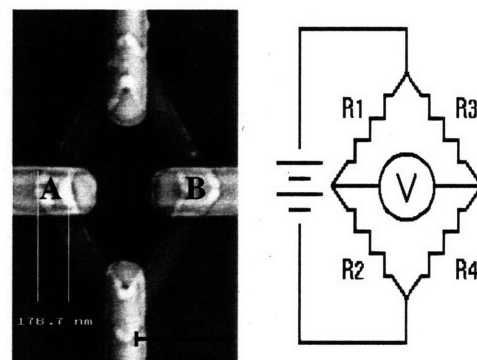


Figure 7. Electrical Representation of Wheatstone Bridge Device. An SEM image of a rhombic PSV device and a circuit diagram of the wheatstone bridge are compared.

PSV devices, small changes in magnetoresistance can be sensed with a high degree of accuracy. However, there are some drawbacks to using this configuration alone, as it can only report relative differences in resistances, and not the actual resistances themselves. This problem could manifest itself in trying to determine the meaning of a negative GMR ratio. However, using our knowledge of device operation we can more readily interpret the data. Since we know that resistance around the rings is minimized at saturation, it can only rise upon switching the field. Therefore, large positive or negative jumps in GMR ratio simply correspond to one half of the ring (one path) increasing resistance relative to its counterpart. Determining which branch causes a positive/negative shift depends on the polarity of the voltage readout across the rings. In our experiments, polarity is not considered; however, it is crucial to understand that a spike or plateau in GMR for one of these devices corresponds to a disturbance in symmetry between branches of the device.

5.2. WHEATSTONE BRIDGE RESULTS

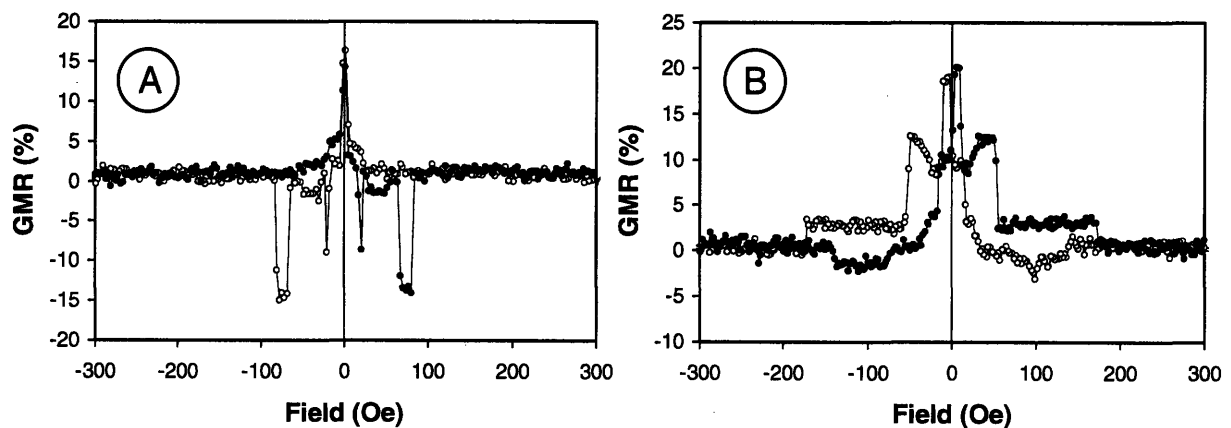


Figure 8. Experimental Results from Wheatstone Bridge Experiments. In A, a GMR loop of the PSV rhombic magnetic ring is shown for magnetization along the easy axis. In B, a GMR loop for the same device only with magnetization along the hard axis is presented to show differences in underlying interactions and sensing abilities.

Shown in Fig. 8 are magnetoresistance loops for multilayer rhombic devices contacted in a wheatstone bridge configuration. This contact configuration yields a GMR ratio that is upwards of 20% as opposed to 1% in classical configuration. An increase in GMR makes the devices more attractive for practical applications, because it is easier to detect individual states when they are spaced over a larger GMR. The external applied magnetic field is along the easy axis in A and along the hard axis in B.

In A, the magnetization runs along the easy axis, causing GMR spikes in resistance to occur at transition points in magnetic field direction. Upon switching the magnetic field, we see a positive spike, implying that a large asymmetry of the circuit has occurred. This would most likely be the result of the NiFe layer transitioning to a vortex state at low field on its way to reverse onion. We can see from A that the NiFe layer transitions quickly to a $\frac{3}{4}$ - $\frac{1}{4}$ configuration (seen as a slightly negative perturbation plateau) at ~25 Oe, and then to its reverse onion state at ~50 Oe, bringing the GMR back to 0. At approximately 70 Oe, the Co layer enters a vortex state of the same direction as the preceding NiFe vortex, with the NiFe in the reverse onion state. This change switches the polarity of the resistance perturbation, continuing until the Co layer reverses as well, returning to a symmetrical circuit and 0 resistance.

Figure 8B shows the MR loop for the wheatstone bridge configuration, with magnetic field traveling along the hard axis, a 90° rotation from A. In this case, we see an even higher GMR ratio than when evaluating the easy axis. As the field passes 0, the resistance reaches a maximum, switching for only a short range of field. Shortly thereafter, it switches to the $\frac{3}{4}$ and $\frac{1}{4}$ configuration. Then, we see a stable drop in GMR (near-symmetry), on its way back to total symmetry. This data already reveals a great

deal about multilayer rhombic devices; however, even more can be deduced if we use this information in conjunction with its classical counterpart.

5.3. CORRELATION BETWEEN MODELS

Similar rhombic structures were tested with two different contact configurations, shown in Fig. 9. Both contact configurations detect shifts in the PSV structure. They also give us more information on what is happening within the device during each transition. For example, when the permalloy layer is in its $\frac{3}{4} - \frac{1}{4}$ state, the resistance shows a strong plateau in classical configuration, however, in the wheatstone bridge configuration, we see a sloped line for this region, implying that the resistance asymmetry within the ring is increasing, most likely due to a

reverse domain propagating through the material. This would not be detected in the classical configuration, because the relative resistance difference would remain the same;

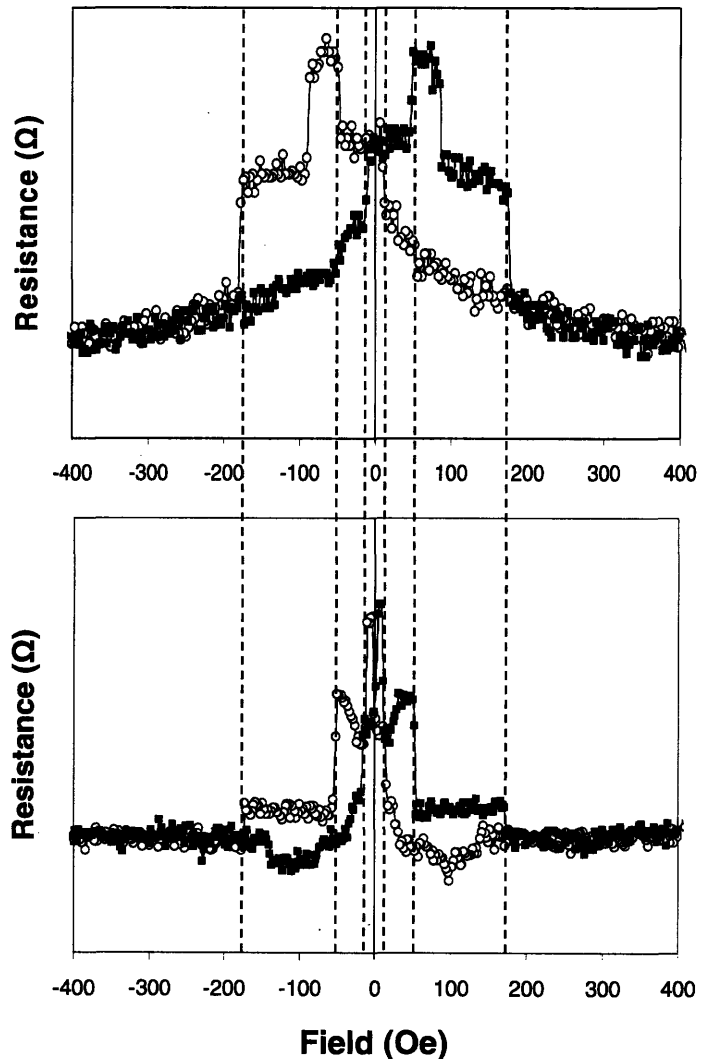


Figure 9. Relative Resistance Correlations Between WB and Classical Experiments. Note that both contact configurations sense changes in the PSV device, only in different ways. As a result, there are advantages and disadvantages to both types of contact configuration.

however, location plays a role in the wheatstone bridge configuration, in some cases, prohibiting it from detection. We now look at the transition where the layers are completely anti-parallel (Co – onion, Py – reverse onion). Co shifts to a vortex state, resulting in an intermediate resistance. This is portrayed as a large jump in classical configuration but absolutely no shift in the wheatstone bridge configuration. In fact, the wheatstone bridge configuration manifests these states as its most shallow plateau. Note, however that in the classical configuration loop, the resistance states fluctuate between 65.4 and 66.1 Ω , whereas the wheatstone bridge configuration fluctuated between 0 and 2 Ω , giving it a much higher GMR ratio, but a lower “true” resistance. These two graphs provide us interesting information about how the shifts occur in the multilayer structure when subject to magnetization across the hard axis.

5.4. CONFIGURATION CHARACTERISTICS

By comparing information from both graphs, we can form logical conclusions on what must be happening inside the ring. At a low switching field, the NiFe seems to enter a very complex state. This causes the maximum shift in GMR for the wheatstone bridge configuration because both paths are resistive in such a way as to cause maximum charge buildup across the two branches. Though the asymmetry causes a spike in the wheatstone configuration, in classical configuration, it is treated as if it were similar to a vortex state. In the easy axis wheatstone bridge configuration, it is safe to assume a vortex state is forming, based on earlier assumptions, but in the hard axis measurements, the symmetry would not be perturbed from a NiFe vortex state.

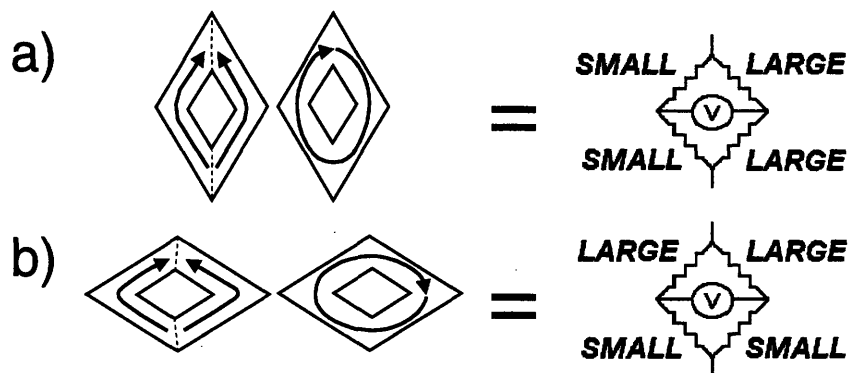


Figure 10. Contact Configuration Effects on Magnetic Moment Sensing. In a), half of the ring has parallel moments, the other half, anti-parallel. In a wheatstone bridge configuration, this will result in asymmetric resistance pathways and a voltage spike. In b), the moments are aligned the same as in a) only along the hard axis. Note that the new effect on the wheatstone bridge configuration is minimal.

Fig. 10 shows that a vortex state in either the NiFe or Co along the hard axis cannot theoretically be accountable for causing a resistance peak/plateau. However, this theory would only work in this configuration, with domain walls pinned to the correct corners of the rhombus, which, in reality, may not occur. In micro-magnetic simulations, these domains seem to grow from multiple corners and migrate towards the center of each leg. At low fields, this may not have had the chance to take place, causing a highly asymmetric state to occur. However, up to a certain point, even symmetrical configurations retain some asymmetry. In Fig. 9, according to the classical configuration, we see a resistance plateau corresponding to a completely anti-parallel alignment of moments, followed by a vortex resistance state. Theoretically, these two states would show up as zero voltage in the wheatstone bridge configuration, however, because of domain wall movement, a slight asymmetry has occurred and stabilized. These domain walls can only hold out until the reversal field is large enough to saturate the ring. This domain wall movement is seen in a sloped plateau on the wheatstone bridge MR loop from ~25-70 Oe. Clearly, the movement has stabilized by the next transition, for the next plateau is stable over a large field, showing the domain walls have been pinned and will

not saturate for a range of fields. Due to the use of both MR loops, we have been able to understand complex interactions taking place during hard-axis magnetization better than by using one alone. Both loops play an important roll in understanding interactions within these devices, however they are only pieces to the puzzle.

6. ANGULAR DEPENDENCE

Preliminary work has been conducted in order to analyze angular dependence (if any) of the switching field in PSV multilayer rhombic devices. The devices underwent major loops in the wheatstone bridge contact configuration with applied field at angles from 0° to 90° off the easy/long axis, incrementing by 10° . In these experiments, at low angles of field (0° - 20°), the resulting GMR loop was nearly identical to that in Fig. 8A. At 30° (two of the four arms of the device are parallel to field), small peaks and plateaus observed in Fig. 8A widen, becoming stable over a larger field, shown in Fig. 11.

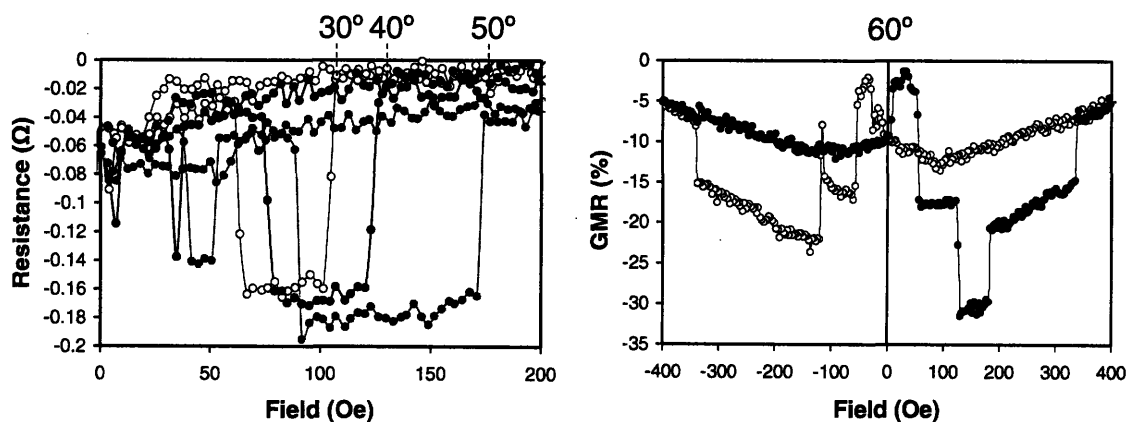


Figure 11. Angular Dependence of Applied Field on PSV Devices. Pseudo spin valve devices with wheatstone bridge contact configuration are magnetized at different angles to see angular effects created. When the angle of magnetization is between 30° and 60° , we see a steady increase in plateau height and width. At 60° , we see a drastic increase in GMR and stability of the ring, possibly attributed to a large portion of the ring being perpendicular to the applied field.

its GMR loop. Note that at 60° , the shape of the loop most resembles that of 90° .

Neglecting polarity, the shear magnitude of induced GMR in the 60° loop is massive, over 30% at some points. This is compared to ~ 20% at 0° and ~ 1% in classical configuration. In addition, the 60° experiment shows stable resistance states over a much broader region of field. At 60°, the device can maintain a stable GMR plateau up to 350 Oe, compared to less than 200 Oe at 90° and less than 100 Oe at 0°. From this preliminary work, it seems that stability can be modified by altering the angle of magnetization. However, further work must be continued to fully understand the magnetic interactions with the device when magnetized at different angles.

7. CONCLUSION

The magnetic switching of multilayer rhombic magnetic rings was explored using two types of contact configurations and a myriad of applied field conditions and angles. Through looking at absolute resistance of rings, we were able to logically determine the underlying magnetic states responsible for corresponding GMR levels. By examining two different contact configurations, we explored the magnetic interactions within these devices, using both graphs to provide us with more information. In addition, we have learned about the advantages and limitations of sensing GMR using these contact configurations, as each has unique characteristics. It was found that pseudo spin valve rhombic multilayer devices exhibit multiple stable states of magnetization that could make them candidates for magnetic materials applications. A number of these states are easily excitable through major magnetization loops. Moreover, through the use of minor loops, we can excite additional states within the device. We proved that both the wheatstone bridge and classical configuration sense similar changes within the device

itself, and that using both configurations together provides more information about the device than using one graph alone. Finally, it has become clear that in order to fully understand rhombic multilayer rings, a great deal of further research must be conducted. It became evident that certain contact configurations provided only a piece of the puzzle when trying to identify interactions within the device. An accurate map of magnetizations within the device must be created in order to fully understand the GMR results obtained through switching. In addition, more research needs to be conducted in exploring angular dependence of the applied field of magnetization. It is possible that an intermediate angle of magnetization may be best for practical applications. Finally, the long term performance and reproducibility of results should be examined before these devices are scaled down for use in commercial applications.

REFERENCES

- ¹ C.A. Ross, F.J. Castano, D. Morecroft, W. Jung, H. Smith, T.A. Moore, T.J. Hayward, J.A.C. Bland, T.J. Bromwich, A.K. Petford-Long. *Mesoscopic thin-film magnetic rings*, Journal of Applied Physics 99, 08S501 (2006).
- ² F.J. Castano, C.A. Ross, C. Frandsen, A. Eilez, D. Gil, H. Smith, M. Redjda, F.B. Humphrey. *Metastable states in magnetic nanorings*, Physical Review B 67, 184425 (2003).
- ³ D. Morecroft, F.J. Castano, W. Jung, J. Feuchtwanger, C.A. Ross. *Influence of contact geometry on the magnetoresistance of elliptical rings*, Applied Physics Letters 88, 172508 (2006).
- ⁴ T.A. Moore, T.J. Hayward, D.H.Y. Tse, J.A.C. Bland, F.J. Castano, C.A. Ross. *Stochastic switching in individual micrometer-sized Permalloy rings*, Physica B 372, 164-167 (2006).
- ⁵ F.J. Castano, C.A. Ross, A. Eilez. *Magnetization reversal in elliptical-ring nanomagnets*, Journal of Physics D: Applied Physics 36, 2031-2035 (2003).
- ⁶ C.A. Ross, F.J. Castano, E. Rodriguez, S. Haratani, B. Vogeli, H. Smith. *Size-dependent switching of multilayer magnetic elements*, Journal of Applied Physics 97, 053902 (2005).
- ⁷ B.A. Everitt, A.V. Pohm, R.S. Beech, A. Fink, J.M. Daughton. *Pseudo Spin Valve MRAM Cells with Sub-Micrometer Critical Dimension*, IEEE Transactions on Magnetics 34, no. 4 (1998).
- ⁸ T.J. Hayward, J. Llandro, R.B. Balsod, J.A.C. Bland, F.J. Castano, D. Morecroft, C.A. Ross. *Reading and writing of vortex circulation in pseudo-spin-valve ring devices*, Applied Physics Letters 89, 112510 (2006).
- ⁹ F.J. Castano, D. Morecroft, W. Jung, C.A. Ross, *Spin-Dependent Scattering in Multilayered Magnetic Rings*, Physical Review Letters 95, 137201 (2005).
- ¹⁰ <http://www.play-hookey.com/digital>
- ¹¹ V.A. Kalinnikov. *Application of Multiple-Valued Logic in Digital Technology (Review)*, Instruments and Experimental Techniques 49, vol. 6, pp. 743-751 (2006).
- ¹² D. Dragoman, M. Dragoman. *Proposal for multiple-valued logic in gated semiconducting carbon nanotubes*, Physica E 33, 178-181 (2006).
- ¹³ <http://www.ternarylogic.com>
- ¹⁴ D.R. Baselt, G.U. Lee, M. Natesan, S.W. Metzger, P.E. Sheehan, R.J. Colton. *A biosensor based on magnetoresistance technology*, Biosensors and Bioelectronics 13, 731-739 (1998).
- ¹⁵ M.M. Miller, G.A. Prinz, S.-F. Cheng, S. Bounnak. *Detection of a micron-sized magnetic sphere using a ring-shaped anisotropic magnetoresistance-based sensor: A model for a magnetoresistance-based biosensor*, Applied Physics Letters 81, no. 12 (2002).
- ¹⁶ E. Saitoh, K. Harii, H. Miyajima, T. Yamaoka, S. Okuma. *Critical phenomena in chiral symmetry breakdown of micromagnetic configurations in a nanostructured ferromagnetic ring*, Physical Review B 71, 172406 (2005)